2008

Can nanotubes display auxetic behaviour?

Yong Tao Yao

Andrew Alderson
University of Bolton, A.Alderson@bolton.ac.uk

K. L. Alderson
University of Bolton, K.Alderson@bolton.ac.uk

Can Nanotubes Display Auxetic Behaviour?

Yong Tao Yao, Andrew Alderson* and Kim Lesley Alderson

Centre for Materials Research and Innovation, The University of Bolton, Deane Rd, Bolton, BL3 5AB, UK.

Received zzz, revised zzz, accepted zzz
Published online zzz (Dates will be provided by the publisher.)

PACS 00.00.Xx, 11.11.Yy, 22.22.Zz, 33.33.Aa (Please insert 4 to 6 PACS codes from the enclosed list or from www.aip.org/pacs)

Corresponding author: email A.Alderson@bolton.ac.uk.

Fully generalised analytical expressions for longitudinal Poisson's ratio are developed for armchair and zigzag Single-Walled Nanotubes (SWNTs) using an energy equivalent approach. Deformation is assumed due to simultaneous bond stretching and bond angle variation in response to an applied axial load. A parametric study is then performed to explore under what circumstances SWNTs may exhibit auxetic (negative Poisson's ratio) response. In principle, auxetic behaviour can be achieved by modifying the hexagonal cell shape to adopt a re-entrant geometry for the case of bond angle variation being the dominant deformation mechanism. Alternatively, altering the length of the characteristic bond oriented in an off-axis direction to below a critical value or modifying the force constants governing the deformation modes so that bond stretching dominates for the conventional hexagonal cell shape can also lead to auxetic behaviour.

1 INTRODUCTION

Nanotubes are essentially macromolecules comprising of atoms (most commonly carbon) arranged on a cylindrical lattice of thickness equal to the size of one atom and having a periodic hexagonal geometry. They can exist as Single-Walled Nanotubes (SWNTs) or as Multi-Walled Nanotubes comprising of nested SWNTs. Since the production of SWNTs in 1991 by Iijima [1], carbon nanotubes have attracted significant attention due to their extreme properties (e.g. thermal, electrical and mechanical). For example, from the mechanical viewpoint, carbon nanotubes have been found to have Young's modulus values typically of the order of 1-2TPa [2-4]. For this reason, carbon SWNTs have clear potential as reinforcing constituents in advanced composite materials [5], for example.

Extreme properties can also be realised through introducing auxetic functionality into a material or structure [6-8]. Auxetic materials are those possessing negative Poisson's ratio behaviour [9]. In other words, they become thicker when stretched and thinner when compressed. Auxetic materials have been shown to lead to enhancements in shear rigidity, plane strain fracture toughness, synclastic curvature upon out-of-plane bending, and fibre pull-out resistance in composites, for example [6-8].

Examples of auxetic materials and structures include honeycombs having tessellating motifs similar to those for nanotubes. Usually a modification leading to a re-entrant ('bow-tie') hexagon cell shape for the honeycomb is considered for auxetic behaviour since this is the geometry under which flexure (usually dominant) or rotation of the cell walls produces the auxetic effect [10-12]. However, auxetic behaviour can also be achieved for the conventional hexagonal honeycomb geometry if stretching of the cell walls dominates the deformation response [10-12].

Given the geometrical similarities then, in the search for extreme properties of materials, it is interesting to consider whether or not nanotubes exhibiting auxetic behaviour are feasible.

Modelling approaches that have been adopted to predict SWNT Poisson's ratio include: Molecular Dynamics [5]; Molecular Mechanics [13]; and analytical approaches based on geometry [14], lattice-dynamics [15] and energy equivalent considerations bridging molecular mechanics and continuum mechanics [16-18]. Finite Element modelling and an analytical model based on beam flexing have been employed to model the Poisson's ratio of tubular truss-like structures having the tessellating hexagon motif [19].

Of these modelling studies, Jindal and Jindal refer to the possibility of negative Poisson's ratio response in carbon SWNTs if the bonds can be made sufficiently flexible [14]. Scarpa et al predict auxetic response for a tubular honeycomb structure having the re-entrant hexagon cell shape [19], consistent with the previous report of an auxetic microfabricated tube having a similar honeycomb geometry [20]. A detailed study of the conditions under which SWNTs may exhibit auxetic behaviour has not, however, been performed to date.

This paper reports a detailed parametric investigation into the Poisson's ratios of SWNTs. The energy equivalent approach of Shen and Li [17] is extended to consider generalised armchair and zigzag SWNTs and the circumstances under which the generalised analytical model predicts auxetic behaviour is explored.

2 SINGLE-WALLED NANOTUBE GEOMETRY

A SWNT is formed by rolling a honeycomb sheet composed of hexagonal cells into a hollow cylinder (Figs. 1a and 1b).

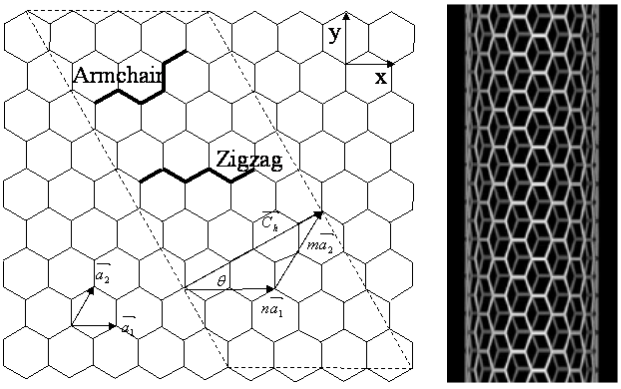

Figure 1. (a) Flat hexagonal honeycomb sheet and coordinate system; (b) armchair SWNT.

Each honeycomb cell wall comprises a bond between a pair of atoms located at the cell wall junctions. The chirality of the SWNT is determined by the axis around which the sheet is rolled into the tube structure. Accordingly, it is usual to define a chiral vector:

$$\vec{C}_h = n\vec{a}_1 + m\vec{a}_2 \tag{1}$$

where $\vec{a}_1$ and $\vec{a}_2$ are unit vectors of the sheet in real space, and n and m are integers denoting the number of unit vectors along the two directions in the honeycomb (Fig. 1a). The chiral angle θ is the angle of the chiral vector with respect to the global x direction. The helicity of the nanotube is defined by the pair of chiral vector integers (n,m) leading to three distinct nanotube structures: armchair (n = m), zigzag (m = 0) and chiral (n ≠ m). Figure 1b, therefore, corresponds to an armchair SWNT.

In this paper, we consider analytical expressions for the Poisson's ratios associated with armchair and zigzag SWNTs. The approach used is that adopted in previous analytical models for auxetic behaviour in cellular structures, and also adopted by Shen and Li [17] and Wu et al [18] specifically for nanotubes. The derivation of the analytical expressions is included here for completeness, and the expressions themselves are thus natural extensions of the expressions developed in refs. [17] and [18] to a generalized nanotube structure in which bond lengths a and b are allowed to differ and α is allowed to assume values other than 120° (Figs. 2 and 3 below).

3 ANALYTICAL MODEL

3.1 Poisson's ratio of an armchair SWNT Figure 2 shows a representative segment of the armchair SWNT. Horizontal (length a) and diagonal (length b) bonds connect atoms to form the nanotube structure. The bond angle between a bond of length a and a bond of length b is β, and the angle between two bonds of length b is α.

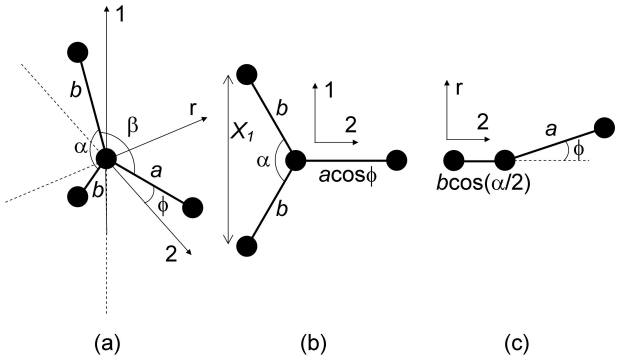

Figure 2. Segment of the bond structure of an armchair SWNT: (a) 3D representation; (b) projection in 1-2 plane; (c) projection in r-2 plane.

The segment length, X_1, in the axial (1-) direction is given by,

$$X_1 = 2b\sin\left(\frac{\alpha}{2}\right) \tag{2}$$

The change in X_1 due to an applied load is given by,

$$\begin{aligned} \mathrm{d}X_1 &= \frac{\partial X_1}{\partial b}\mathrm{d}b + \frac{\partial X_1}{\partial \alpha}\mathrm{d}\alpha \\ &= 2\left[\sin\left(\frac{\alpha}{2}\right)db + \frac{b}{2}\cos\left(\frac{\alpha}{2}\right)d\alpha\right] \end{aligned} \tag{3}$$

and so the strain in the axial direction is

$$\varepsilon_1 = \frac{dX_1}{X_1} = \frac{\sin\left(\frac{\alpha}{2}\right)db + \frac{b}{2}\cos\left(\frac{\alpha}{2}\right)d\alpha}{b\sin\left(\frac{\alpha}{2}\right)} \tag{4}$$

Similarly, the segment length (X_2) in the transverse plane of the nanotube is given by,

$$X_2 = \left[a + b\cos\left(\frac{\alpha}{2}\right)\right] \tag{5}$$

The change in X_2 due to an applied load is given by,

$$\begin{aligned} \mathrm{d}X_2 &= \frac{\partial X_2}{\partial a}\mathrm{d}a + \frac{\partial X_2}{\partial b}\mathrm{d}b + \frac{\partial X_2}{\partial \alpha}\mathrm{d}\alpha \\ &= \left[\mathrm{d}a + \cos\left(\frac{\alpha}{2}\right)\mathrm{d}b - \frac{b}{2}\sin\left(\frac{\alpha}{2}\right)\mathrm{d}\alpha \right] \end{aligned} \tag{6}$$

and so the circumferential strain is

$$\varepsilon_2 = \frac{dX_2}{X_2} = \frac{da + \cos\left(\frac{\alpha}{2}\right)db - \frac{b}{2}\sin\left(\frac{\alpha}{2}\right)d\alpha}{a + b\cos\left(\frac{\alpha}{2}\right)} \tag{7}$$

We consider bond stretching and bond angle variation to be the deformation modes acting. In other words, non-bond interactions and the like are ignored in this treatment.

Consider first, bond stretching in response to a load applied along the axial (1-) direction.

There are two bonds of length b, and one of length a in the representative segment. Hence, the potential energy of the segment due to bond stretching, U_s, is given by,

$$U_s = \frac{1}{2}C_a(da)^2 + 2\left[\frac{1}{2}C_b(db)^2\right] \tag{8}$$

where C_a and C_b are the bond stretching force constants for bonds of length a and b, respectively.

In this case there is no component of applied force along the bond of length a, i.e.

$$da = 0 \tag{9}$$

The virtual work W_s done by the axial force f due to bond stretching is given by:

$$\frac{W_s}{V} = \frac{1}{2}\sigma_1\varepsilon_1^{(s)} = \frac{1}{2}\frac{f}{A}\left(\frac{1}{X_1}\frac{\partial X_1}{\partial b}db\right) \tag{10}$$

where $\varepsilon_1^{(s)}$ is the strain along the 1- direction due to bond stretching, A is the cross-sectional area of the segment and V (= AX_1) is the segment volume.

From the principle of conservation of energy, $W_s = U_s$ at equilibrium, and so from equations (3), (8)-(10) we get:

$$db = \frac{f}{C_b}\sin\left(\frac{\alpha}{2}\right) \tag{11}$$

Now consider bond angle variation in response to a load applied along the axial (1-) direction.

The potential energy of the segment due to bond angle variation, U_a, is given by,

$$U_a = 2\left[\frac{1}{2}C_\alpha(d\alpha)^2\right] + 4\left[\frac{1}{2}C_\beta(d\beta)^2\right] \tag{12}$$

where C_α and C_β are the bond angle variation force constants for bond angles α and β, respectively.

For the armchair nanotube, angles α and β are related by

$$\cos\beta = -\cos\phi\cos\left(\frac{\alpha}{2}\right) \tag{13}$$

where ϕ (= $\pi/2n$) is the angle between the bond of length a and the b-b plane (Fig. 2) and which remains constant for loading along the axial direction.

Differentiating equation (13), one obtains

$$d\beta = \frac{\tan\left(\frac{\alpha}{2}\right)}{2\tan\beta}d\alpha \tag{14}$$

The virtual work W_a done by the axial force f due to bond angle variation is given by:

$$\frac{W_a}{V} = \frac{1}{2}\sigma_1\varepsilon_1^{(a)} = \frac{1}{2}\frac{f}{A}\left(\frac{1}{X_1}\frac{\partial X_1}{\partial \alpha}d\alpha\right) \tag{15}$$

where $\varepsilon_1^{(a)}$ is the strain along the 1- direction due to bond angle variation.

From the principle of conservation of energy, $W_a = U_a$ at equilibrium, and so from equations (3), (12), (14) and (15) we get:

$$d\alpha = \frac{fb}{2\left(C_\alpha + \delta C_\beta\right)}\cos\left(\frac{\alpha}{2}\right) \tag{16}$$

where

$$\delta = \frac{\tan^2\left(\frac{\alpha}{2}\right)}{2\tan^2\beta} \tag{17}$$

The longitudinal Poisson's ratio of a tube is defined by

$$\nu_{12} = -\frac{\varepsilon_2}{\varepsilon_1} \tag{18}$$

Substituting equations (9), (11) and (16) into equations (4) and (7) provides expressions for the strains to be employed in equation (18), yielding the following expression for the longitudinal Poisson's ratio of the armchair SWNT

$$\nu_{12} = \frac{\cos\left(\frac{\alpha}{2}\right)\left[\frac{b^2C_b}{4\left(C_\alpha + \delta C_\beta\right)} - 1\right]}{\left[\frac{a}{b} + \cos\left(\frac{\alpha}{2}\right)\right]\left[\frac{b^2C_b}{4\left(C_\alpha + \delta C_\beta\right)\tan^2\left(\frac{\alpha}{2}\right)} + 1\right]} \tag{19}$$

3.2 Poisson's ratio of a zigzag SWNT Figure 3 shows a representative segment of the zigzag SWNT.

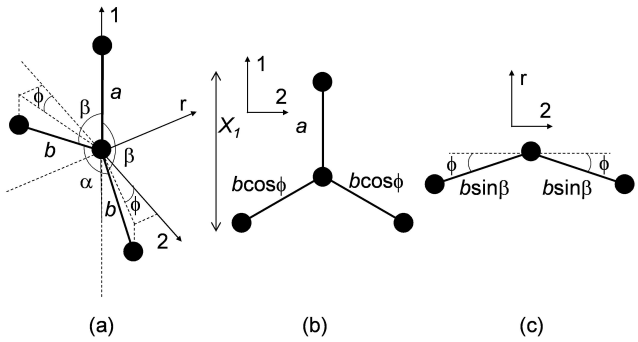

Figure 3. Segment of the bond structure of a zigzag SWNT: (a) 3D representation; (b) projection in 1-2 plane; (c) projection in r-2 plane.

In this case, the segment length, X_1, in the axial direction is given by,

$$X_1 = a - b\cos\beta \tag{20}$$

The change in X_1 due to an applied load is given by,

$$\mathrm{d}X_1 = \mathrm{d}a - \cos\beta\mathrm{d}b + b\sin\beta\mathrm{d}\beta \tag{21}$$

Similarly, the segment length (X_2) in the transverse plane is given by,

$$X_2 = 2b\sin\beta \tag{22}$$

and

$$\mathrm{d}X_2 = 2\left(\sin\beta\mathrm{d}b + b\cos\beta\mathrm{d}\beta\right) \tag{23}$$

For the zigzag nanotube, angles α and β are related by

$$\sin\beta = \frac{\sin\left(\frac{\alpha}{2}\right)}{\cos\phi} \tag{24}$$

where ϕ (= π/2n) is the angle defined in Fig. 3 and which remains constant for loading along the axial direction.

Following the method described in the previous subsection, the changes in the 3 independent variables required to determine the mechanical properties of the zigzag SWNT under axial loading are found to be:

$$\mathrm{d}a = \frac{f}{C_a} \tag{25}$$

$$\mathrm{d}b = -\frac{f\cos\beta}{2C_b} \tag{26}$$

$$\mathrm{d}\beta = \frac{fb\sin\beta}{4\left(4\delta C_\alpha + C_\beta\right)} \tag{27}$$

The expression thus derived for the longitudinal Poisson's ratio of the zigzag SWNT is:

$$\nu_{12} = \frac{\cos\beta\left(\frac{a}{b} - \cos\beta\right)\left[1 - \frac{b^2 C_b}{2\left(4\delta C_\alpha + C_\beta\right)}\right]}{\left[\frac{2C_b}{C_a} + \cos^2\beta + \frac{b^2 C_b \sin^2\beta}{2\left(4\delta C_\alpha + C_\beta\right)}\right]} \tag{28}$$

4 RESULTS

Equations (19) and (28) indicate that the longitudinal Poisson's ratios for the armchair and zigzag SWNTs, respectively, are dependent on the chiral vector integer, bond lengths, bond angles and the associated force constants with these internal geometrical parameters. In the following, we explore the dependency of the longitudinal SWNT Poisson's ratios on these parameters, with particular reference to the search for auxetic functionality in nanotube systems.

A 'standard' SWNT parameter set is defined: $a = b =$ 0.142nm, $\alpha = 120°$, $C_a = C_b = 742$ nN nm^{-1} and $C_\alpha = C_\beta =$ 1.42 nN nm, which are appropriate parameters for carbon nanotubes [17]. A standard value of $n = 12$ is also defined. The effect of varying any one parameter (or ratio of parameters) whilst holding all other parameters at their standard values is explored.

4.1 Geometry variations The variation of the longitudinal Poisson's ratios as a function of n and nanotube diameter is shown in Figs. 4a and 4b, respectively. The general trend is for ν_L to decrease smoothly towards the value precited for graphite as the diameter increases. For any given value of n the zigzag SWNT displays a slightly larger value of ν_L than the armchair SWNT, although the curves for the two configurations almost completely overlap when plotted against diameter. ν_L is positive for all n in this case.

The variation in ν_L for the armchair SWNT with angle α is shown in Fig. 5a, for n = 4, 12, 250 and ∞. The value of n is seen to have little effect on the ν_L versus α trends until $\alpha \rightarrow 360°$, whereupon the magnitude of ν_L decreases as n increases. For $0 < \alpha < 180°$, ν_L increases from an initially zero value at 0° to a maximum positive value at around 120-140° before returning to zero at 180°. ν_L is negative for $180 < \alpha < 360°$, increasing in magnitude as α increases.

In the case of the zigzag SWNT there exists a range of α which is not physically possible for the given bond dimensions. The inaccessible range of α is determined from equation (24) when β = 90°. For the case of n = 12, the zigzag SWNT cannot be constructed for $165 < \alpha < 195°$ when $a = b$. Consequently, there is a gap in the ν_L versus α prediction in Fig. 5b for the zigzag SWNT. For $0 < \alpha <$ 165°, ν_L decreases from an initial value of ~+0.5 at 0° to zero at 165°. Auxetic behaviour is predicted for $195 < \alpha <$ 360°, increasing in magnitude from 0 at $\alpha = 195°$ to a maximum magnitude at $\alpha \sim 240°$, before returning to zero as $\alpha \rightarrow 360°$. The magnitude of the negative Poisson's ratio is much smaller over the same interval of α for the zigzag SWNT than for the armchair SWNT.

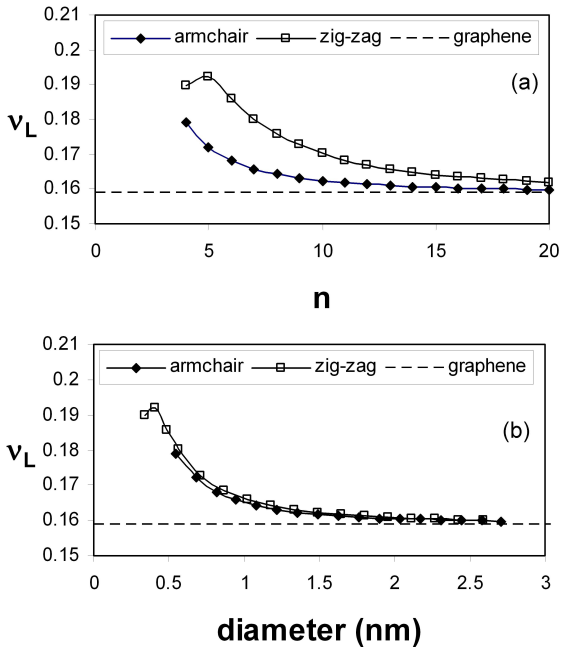

Figure 4. (a) Longitudinal Poisson's ratio ν_L vs chiral vector integer n; (b) ν_L vs SWNT diameter ($=2n\left[a+b\cos\left(\alpha/2\right)\right]/\pi$ for the armchair SWNT and $2nb\sin\beta/\pi$ for the zigzag SWNT). Calculations employed $a = b = 0.142$nm, $\alpha = 120°$, $C_a = C_b = 742$ nN nm^{-1} and $C_\alpha = C_\beta = 1.42$ nN nm.

A smoothly decreasing and linearly increasing positive ν_L is predicted as the bond length a increases for the armchair and zigzag configurations, respectively (Fig. 6a). Variation of a cannot lead to auxetic behaviour for the standard values of the other geometrical and force constant parameters used in the model.

Variation of bond length b, on the other hand, can lead to auxetic behaviour for all other parameters assuming standard values (Fig. 6b). The range for auxetic behaviour for both armchair and zigzag SWNTs in this case is $b <$ 0.11nm. As $b \rightarrow 0$nm, $\nu_L \rightarrow 0$ and ∞ for the armchair and zigzag configurations, respectively. Increasing b from 0 leads to an increase in the magnitude of the negative ν_L for the armchair SWNT until a maximum magnitude is reached at around b ~0.055nm, before returning towards zero and then positive values (above b ~ 0.11nm) as b increases further. A rapid increase in ν_L is observed as b increases in the low b range ($b <$ 0.03nm) for the zigzag SWNT, before assuming a shallower increase with increasing b thereafter.

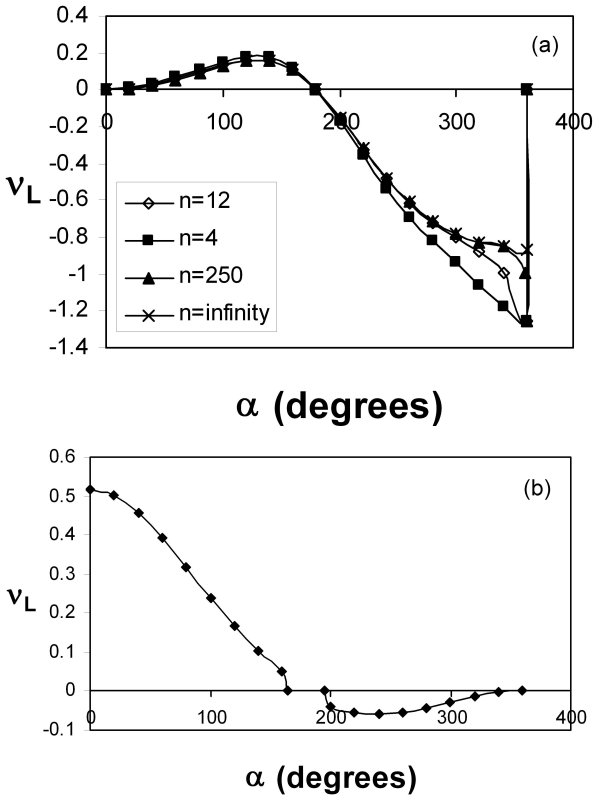

Figure 5. (a) Longitudinal Poisson's ratio ν_L vs bond angle α for the armchair SWNT having n values of 4, 12, 250 and ∞. (b) ν_L vs α for the zigzag SWNT (n = 12). Calculations employed $a = b$ = 0.142nm, $C_a = C_b = 742$ nN nm^{-1} and $C_\alpha = C_\beta = 1.42$ nN nm.

4.2 Force constant variations Figure 7a shows that auxetic behaviour can be predicted through variation of the bond-stretch to bond-angle-variation force constant ratio (C_b/C_α). In Fig. 7a $C_b = C_a$ and $C_\alpha = C_\beta$, and C_α (C_β) is fixed at the standard value as C_b (C_a) is varied. The curves for the armchair and zigzag SWNTs overlap closely. ν_L tends to the values for pure bond stretching and bond angle variation (hinging) as $C_b/C_\alpha \rightarrow 0$ and ∞, respectively. Auxetic behaviour is predicted when $C_b/C_\alpha < 300$ nm^{-2}.

Auxetic behaviour is not predicted when varying the ratio of the two bond-stretch force constants (C_b/C_a) through varying C_a (Fig. 7b). ν_L is independent of C_b/C_a for the armchair SWNT. For the zigzag SWNT, ν_L initially decreases rapidly from a maximum positive value of ν_L = +0.37 at $C_b/C_a = 0$ before tailing off towards zero as $C_b/C_a \rightarrow \infty$.

For the case of varying the bond-angle-variation force constant ratio (C_β/C_α) through varying C_β (Fig. 7c) the trends for the armchair and zigzag SWNTs closely overlap. Both positive and negative values of ν_L can be predicted, with ν_L decreasing in a smooth non-linear manner as C_β/C_α in-

creases: $0 < \nu_L < 0.3$ when $0 < C_\beta/C_\alpha < 3.3$; and $-0.33 < \nu_L < 0$ when $3.3 < C_\beta/C_\alpha < \infty$.

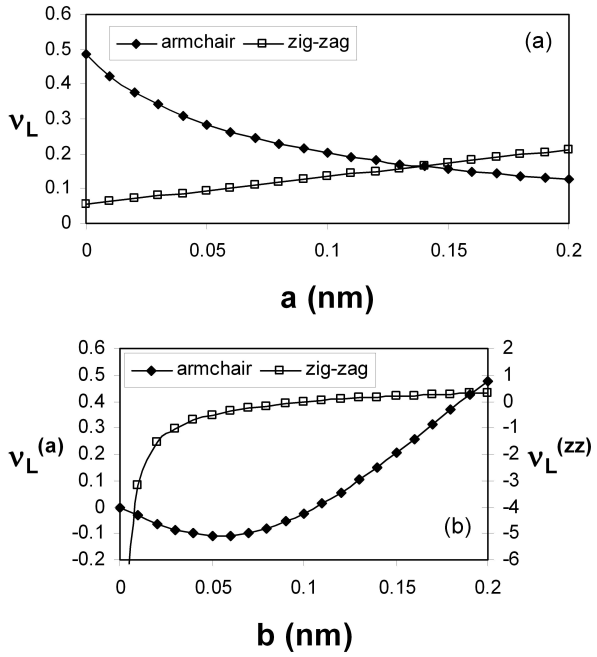

Figure 6. (a) Longitudinal Poisson's ratio ν_L vs bond length a for the armchair and zigzag SWNTs having $b = 0.142$nm. (b) ν_L vs b for the armchair ($\nu_L^{(a)}$) and zigzag ($\nu_L^{(zz)}$) SWNTs ($a = 0.142$nm). Calculations employed $n = 12$, $\alpha = 120°$, $C_a = C_b = 742$ nN nm^{-1} and $C_\alpha = C_\beta = 1.42$ nN nm.

5 DISCUSSION

In this paper we have reported the development of a generalised analytical model for the prediction of the longitudinal Poisson's ratios of armchair and zigzag SWNTs. The model considers only bond stretching and bond angle variation as deformation mechanisms, and allows the variation of geometrical and force constant parameters from those known to exist for carbon SWNTs to be explored in the search for auxetic behvaviour in such systems.

The longitudinal Poisson's ratio is predicted in this model to be dependent on the SWNT diameter (Fig. 4b), which is itself determined by the value of the chiral vector integer n (Fig. 4a). The general trend of a positive Poisson's ratio decreasing with increasing SWNT diameter towards a limiting lower value at infinite diameter is consistent with the trend predicted from Molecular Mechanics simulations [13] and other analytical models for carbon SWNTs, e.g the energy-based models developed by Shen and Li [17] and Wu et al [18]. In fact equations (19) and (28) reduce to the expressions derived by Shen and Li when $a = b$, $C_a = C_b = C_p$, and $C_\alpha = C_\beta = C_\theta$.

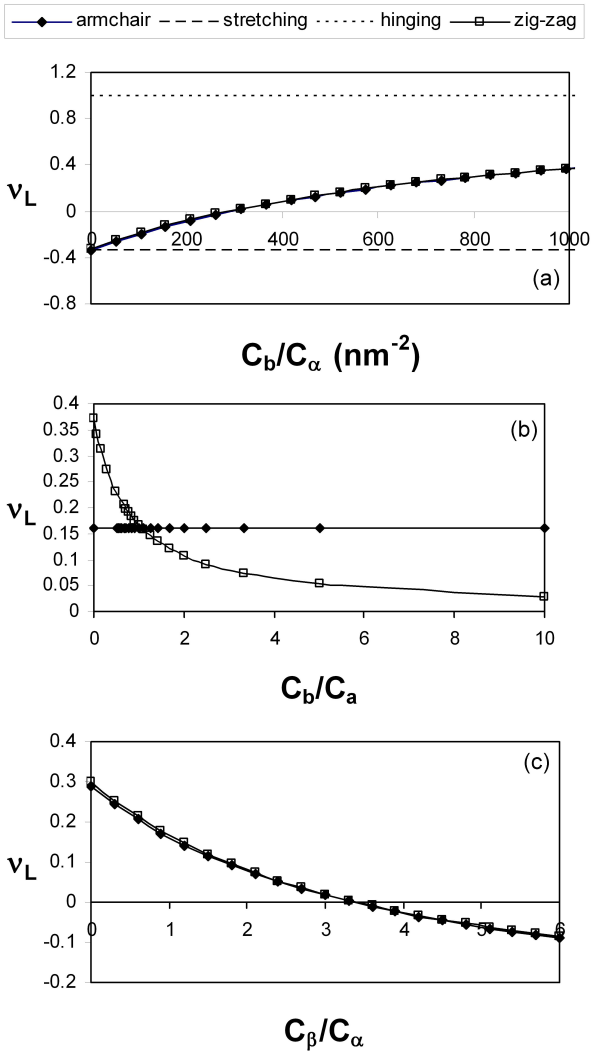

Figure 7. (a) ν_L vs the bond stretch-to-bond angle variation force constant ratio (C_b/C_α) for the armchair and zigzag SWNTs, with $C_b = C_a$ and $C_\alpha = C_\beta = 1.42$ nN nm employed in the calculations. (b) ν_L vs the bond stretch force constant ratio (C_b/C_a) for the armchair and zigzag SWNTs, employing $C_b = 742$ nN nm^{-1} and $C_\alpha = C_\beta = 1.42$ nN nm in the calculations. (c) ν_L vs the bond angle variation force constant ratio (C_β/C_α) for the armchair and zigzag SWNTs, employing $C_a = C_b = 742$ nN nm^{-1} and $C_\alpha = 1.42$ nN nm in the calculations. All calculations employed $n = 12$, $a = b = 0.142$nm and $\alpha = 120°$.

The armchair SWNT trend is also in agreement with that predicted by Popov et al who developed analytical expressions within a lattice-dynamics approach [15]. However, the zigzag SWNT trend predicted by Popov et al is contrary to that predicted by the model presented here in that it predicts a smooth non-linear increase towards a limiting value for the (positive) Poisson's ratio with increasing diameter. The Molecular Dynamics simulations performed by Suzuki and Nomura predict trends similar to the Popov zigzag trends for both zigzag and armchair SWNTs [5].

Jindal and Jindal have used a purely geometrical approach to develop expressions for the longitudinal Poisson's ratio of SWNTs undergoing deformation due to bond stretching and bond angle variation [14] and predict that the Poisson's ratio is dependent on the chirality of the SWNT, but is independent of nanotube diameter for a given chirality.

The ν_L trends with bond angle are similar to those predicted for a flat sheet ($n = \infty$) having otherwise identical geometrical and force constant parameters (Fig. 5a). The effect of tube diameter appears to lead to the largest variation from the flat sheet prediction at high values of α. Analytical models for flat honeycombs deforming by concurrent flexure, hinging and stretching of the honeycomb ribs have been developed previously [10-12]. The SWNT expressions developed in this paper reduce to the concurrent analytical model expressions when $n = \infty$ in the SWNT expressions (equations (19) and (28)) and the flexure force constant in the flat sheet expressions is set to infinity.

Tubular truss-like structures having the hexagonal motif have been modelled using the Finite Element (FE) method and analytically assuming rib flexure as the deformation mechanism [19]. Rib flexure has previously been shown to give identical analytical expressions for Poisson's ratio as rib hinging (angle variation) [10,11]. The ν_L dependencies on bond angle for both the armchair and zigzag SWNTs predicted in this paper are consistent with those predicted as a function of rib angle in the tubular truss-like structures.

Variation of bond length a is not predicted to lead to auxetic behaviour for the conventional hexagon cell shape (Fig. 6a). The predicted ν_L trends are expected from the inverse proportionality for the armchair, and proportional relationship for the zigzag SWNT with respect to bond length a in equations (19) and (28), respectively.

However, auxetic behaviour is predicted if bond length b can be made sufficiently small (Fig. 6b). The moment causing bond angle variation due to an applied axial load is proportional to the bond length b. Consequently, provided the bond stretch and bond angle variation force parameters remain constant independent of b (as assumed in the calculations of Fig. 6b), then the degree of bond angle variation will decrease as b decreases until such a point that bond stretching becomes the predominant deformation mode. Stretching of the ribs of a conventional honeycomb is known to lead to auxetic behaviour [10-12].

Similar reasoning explains the predicted ν_L vs C_b/C_α trends (Fig. 7a). Low values of C_b/C_α correspond to bond stretching dominating over bond angle variation and, therefore, negative Poisson's ratio response is realised for the conventional honeycomb geometry employed in the calculations of Fig. 7a. For values of C_b/C_α in excess of a critical value ($C_b/C_\alpha \sim 300$ nm^{-2}), then bond angle variation dominates the deformation mechanism leading to positive Poisson's ratio behaviour. This finding is consistent with the SWNT analytical model of Jindal and Jindal [14] which predicted auxetic behaviour for the case of bond lengths becoming sufficiently flexible with respect to bond angle variation.

Bond length a is perpendicular to the axial loading direction for the armchair SWNT and, consequently, there is no component of the applied load acting along the length of bond a with which to cause bond stretching. Hence the longitudinal Poisson's ratio expression for the armchair SWNT (equation (19)) does not contain the bond stretch force constant C_a and, therefore, the predicted ν_L is independent of C_b/C_a when C_a is the variable parameter (Fig. 7b).

For the zigzag SWNT, bond a is aligned along the loading direction. In this case, as $C_a \rightarrow 0$ (i.e. $C_b/C_a \rightarrow \infty$), deformation due to axial tension becomes predominantly one of bond a stretching. In the limiting case of $C_a = 0$, there is no lateral (circumferential) deformation of the cellular structure and so $\nu_L \rightarrow 0$ as $C_b/C_a \rightarrow \infty$ (Fig. 7b). Conversely, as $C_b/C_a \rightarrow 0$ for the zigzag SWNT, bond a becomes inextensible and the Poisson's ratio response is determined by the bond b extension and bond angle variation mechanisms which yield a positive value for ν_L for the parameters employed in the calculation.

Bond angles α and β are dependent variables (equations (13) and (24) for the armchair and zigzag SWNTs, respectively) and so varying the bond angle variation force constant ratio C_β/C_α does not alter the amount of change of one angle with respect to the other under loading. Rather, it alters the amount of bond angle variation with respect to the amount of bond stretching. As $C_\beta/C_\alpha \rightarrow 0$ due to $C_\beta \rightarrow 0$, bond angle variation becomes easier as a whole and more dominant over bond stretching. Hence, ν_L attains its highest positive value when $C_\beta/C_\alpha \rightarrow 0$ due to $C_\beta \rightarrow 0$ for the conventional hexagon cell shape used in the calculations for Fig. 7c. Conversely, as C_β/C_α increases due to increasing C_β, bond angle variation becomes more difficult and there will be a critical value at which bond stretching becomes the dominant deformation mode, leading to auxetic behaviour for higher values of C_β/C_α. The critical value occurs at $C_\beta/C_\alpha \sim 3.4$ in Fig. 7c and $\nu_L \rightarrow -0.33$ (the bond stretching limit) as $C_\beta/C_\alpha \rightarrow \infty$ due to $C_\beta \rightarrow \infty$.

In the above, the developed generalised analytical model for SWNTs possessing a hexagonal honeycomb cell structure has been used to consider under what conditions auxetic behaviour might be realised in principle. In reality it is perhaps difficult to perceive how the re-entrant hexagon motif ($180 < \alpha < 360°$) leading to auxetic behaviour (Fig. 5) can be achieved in, for example, carbon SWNT structures. It is possible that alternative nanohoneycombs may need to be developed in order to produce auxetic

nanotubes based on the re-entrant hexagon cell shape. Examples of possible conventional and re-entrant nanohoneycomb frameworks are shown in Fig. 8, comprising a network of acetylene groups forming the arms of the honeycomb connected at the junctions by benzene rings [9,10]. Molecular mechanics, FE and analytical models have all predicted auxetic behaviour for the network based on the re-entrant sub-unit shown in Fig. 8b [9,10]. From the models developed in this paper, it would be expected that a SWNT comprising the cell structure of Fig. 8b would also be auxetic.

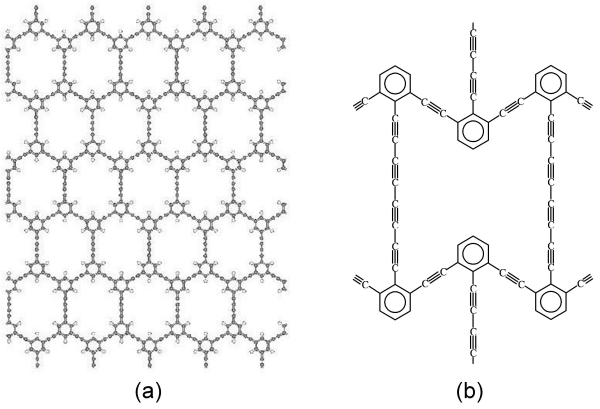

Figure 8. Theoretical nanohoneycombs based on (a) conventional hexagon and (b) re-entrant hexagon tessellating motifs [9,10].

The model has also shown that it may be possible to achieve auxetic behaviour in SWNT structures possessing the conventional ($0 < \alpha < 180°$) hexagon cell shape through variation of bond lengths or force constants. This may possibly be achieved by introducing more than one atomic species into the SWNT (e.g. boron nitride-carbon [$B_xN_yC_z$] hybrid nanotubes [21]). Alternatively, the nanohoneycombs of the type shown in Fig. 8 also offer a route to honeycombs in which the effective 'bond' lengths and force constants can be varied. In this latter case, the force constants represent stretching and angle variation not of single bonds and angles between single bonds, but of 'ribs' of connected bonds and the angles between these ribs, respectively. It has been shown that these latter rib lengths and force constants can be tuned through the number of acetylene groups in the ribs and/or the introduction of benzene rings into the vertical ribs [10].

In principle there is no reason why SWNTs should be restricted to the hexagon cell shape. For example, flat auxetic nanohoneycombs have been proposed having a tessellating triangles topology [22]. The potential to develop auxetic SWNTs does, therefore, appear to be realistic, albeit one possibly still requiring significant advances in chemical synthesis.

6 CONCLUSIONS

A generalised analytical model for the longitudinal Poisson's ratios of armchair and zigzag SWNTs has been developed based on energy equivalent considerations. The model considers bond stretch and bond angle interactions only. A parametric study using the model indicates the Poisson's ratio may be negative under certain geometric and force constant conditions. Auxetic SWNTs are, therefore, possible in principle. The realisation of auxetic SWNTs may require SWNTs having more than one atomic species in order to achieve the required combination of geometric and force constant parameters. Alternatively, other nanohoneycomb structures, based on ribs comprising several bonds rather than single bonds, and possibly having a non-hexagonal cell shape, may be required.

Acknowledgements

YTY has been funded through a doctoral studentship from the Northwest Composites Centre in the UK.

References

[1] S. Iijima, *Nature*, **354**, 56 (1991).
[2] M.M.J. Treacy, T.W. Ebbesen and J.M. Gibson, *Nature*, **381**, 678 (1996)
[3] A. Krishnan, E. Dujardin, T.W. Ebbesen, P.N. Yianilos and M.M.J. Treacy, *Phys. Rev. B.*, **58**, 14013 (1998).
[4] J.P. Salvetat, J.M. Bonard, N.H. Thomson, A.J. Kulik, L. Forro, W. Benoit and L. Zuppiroli, *Appl. Phys. A.*, **69**, 255 (1999).
[5] K. Suzuki, S. Nomura, *J. Comp. Matls.*, **41**, 1123 (2007).
[6] R.S. Lakes, *Science*, **235**, 1038 (1987).
[7] K.E. Evans, *Chem. Ind.* **20**, 654 (1990).
[8] A. Alderson and K. Alderson, *Proc. Inst. Mech. Eng., Part G, J. Aero. Eng.,* **221**, 565 (2007).
[9] K.E. Evans, M.A. Nkansah, I.J. Hutchinson and S.C. Rogers, *Nature*, **353**, 124 (1991).
[10] K.E. Evans, A. Alderson and F.R.Christian, *J. Chem. Soc. Faraday Trans.,* **91(16)**, 2671 (1995).
[11] I.G. Masters and K.E. Evans, *Compos. Struct.,* **35**, 403 (1997).
[12] J.P.M. Whitty, F. Nazare, A. Alderson, *Cellular Polymers*, **21(2)**, 69 (2002).
[13] S. Xiao and W. Hou, *Fullerenes, Nanotubes, and Carbon Nanostructures*, **14**, 9 (2006).
[14] P. Jindal and V.K. Jindal, *Journal of Computational and Theoretical Nanoscience*, **3(1)**, 148 (2006).
[15] V.N. Popov, V.E. Van Doren and M. Balkanski, *Phys. Rev. B*, **61**, 3078 (2000).
[16] T. Natsuki, K. Tantrakarn and M. Endo, *Carbon*, **42**, 39 (2004).
[17] L. Shen and J. Li, *Phys. Rev. B*, **69**, 045414 (2004).
[18] Y. Wu, X. Zhang, A.Y.T. Leung and W. Zhong, *Thin-Walled Structures*, **44**, 667 (2006).
[19] F. Scarpa, C.W. Smith, M. Ruzzene and M.K. Wadee, *Phys. Stat. Sol. B*, **245(3)**, 584 (2008).

[20] R.J. Jackman, S.T. Brittain, A. Adams, M.G. Prentiss and G.M. Whitesides, *Science*, **280**, 2089 (1998).
[21] C. Goze, L. Vaccarini, L. Henrard, P. Bernier, E. Hernandez and A. Rubio, *Synthetic Metals*, **103**, 2500 (1999).
[22] J.N. Grima, A. Alderson, K.E. Evans, *Phys. Stat. Sol. B*, **242(3)** 561 (2005).